

CrystEngComm

Accepted Manuscript



This is an *Accepted Manuscript*, which has been through the Royal Society of Chemistry peer review process and has been accepted for publication.

Accepted Manuscripts are published online shortly after acceptance, before technical editing, formatting and proof reading. Using this free service, authors can make their results available to the community, in citable form, before we publish the edited article. We will replace this *Accepted Manuscript* with the edited and formatted *Advance Article* as soon as it is available.

You can find more information about *Accepted Manuscripts* in the [Information for Authors](#).

Please note that technical editing may introduce minor changes to the text and/or graphics, which may alter content. The journal's standard [Terms & Conditions](#) and the [Ethical guidelines](#) still apply. In no event shall the Royal Society of Chemistry be held responsible for any errors or omissions in this *Accepted Manuscript* or any consequences arising from the use of any information it contains.

Positions of Amino Groups in Ammonium Salts Turn the Conformations of Crown Ethers: Crystal Structure, Hirshfeld Surfaces and Spectroscopic Studies

Yang-Hui Luo,^a Dong-En Wu,^a Wen-Tao Song,^a Shu-Wang Ge^a and Bai-Wang Sun*^a

ABSTRACT: Six supramolecular assembly complexes: pyridine-4-ammonium-18-crown-6-perchlorate ($[(C_5H_7N_2)_2 \cdot (18-C-6)]^{2+} \cdot 2(ClO_4)^-$, **1**), 2-chloride-pyridine-3-ammonium-18-crown-6-perchlorate ($[(C_5H_6N_2Cl) \cdot (18-C-6)]^+ \cdot (ClO_4)^-$, **2**), isoniazide-ammonium-18-crown-6-tetrafluoroborate ($[(C_6H_9N_3O)_2 \cdot (18-C-6)_3]^{4+} \cdot 4(BF_4)^- \cdot 4(H_2O)$, **3**), naphthylammonium-18-crown-6-tetrafluoroborate ($[(C_{10}H_{10}N) \cdot (18-C-6)]^+ \cdot (BF_4)^-$, **4**), benzidine-ammonium-15-crown-5-tetrafluoroborate ($[(C_{12}H_{14}N_2) \cdot (15-C-5)_2]^{2+} \cdot 2(BF_4)^-$, **5**), salicylamide-18-crown-6-tetrafluoroborate ($[(C_7H_6NO_2BF_2) \cdot (18-C-6)]$, **6**) have been prepared and investigated detailed by single-crystal X-ray diffraction, Hirshfeld surfaces analysis, Raman and IR spectra in this work. The position of amino group on ammonium salt plays a key role in the supramolecular structure and conformation of crown ethers: **1** and **3** formed five- and nine-member pendulum-like structures, respectively; **2** and **4** formed umbrella-like structures; **5** formed “dumbbell-like” structure with 15-crown-5; salicylamide in **6** formed a novel complex with tetrafluoroboric acid. The 18-crown-6 molecule displays “round” “ D_{3d} like” conformation in **1** and **6** while display “boat-form” in **2** and **4**, and display two different conformations in **3** with “round” “ D_{3d} like” and “chair-like” conformations in stoichiometric of 2:1. The change of conformations makes a significant difference on intermolecular interactions and spectroscopic properties: the “ D_{3d} like” is more apt to H-H and O-H contacts than “chair-like”, the latter is apt to C-H... π contacts; in the presences of ammonium salts, the characteristic Raman peaks at 418 cm^{-1} and within $900\text{-}800\text{ cm}^{-1}$ are maintained for “ D_{3d} like” while vanished for “boat-form” and “chair-like”, the characteristic IR peak within the region $1130\text{-}1090\text{ cm}^{-1}$ was narrowed down for “ D_{3d} like” while broadened for other two conformations

■ INTRODUCTION

As their undeniable importance in the development of supramolecular and host-guest chemistry, crown ethers have been the subject of various studies in supramolecular chemistry and crystal engineering in recent years,¹⁻⁵ especially for the investigation of host-guest interactions in the construction of supramolecular architectures.⁶⁻¹⁰ The host-guest interaction between crown ethers and guest molecules is an important secondary interaction not only mimicking the natural systems but also constructing new materials.¹¹⁻¹⁴ Crown ethers usually acted as macrocyclic hosts for alkali and transition-metal ions complexing, or served as building blocks to create a variety of molecularly assembled architectures with such complementary guest molecules as hydrogenate cations, organic salts and other species.¹⁵⁻¹⁸ To date, numerous artificial complexes of crown ethers with guest molecules via host-guest interactions have been developed for supramolecular polymers with some promising properties due to their good selectivity, high efficiency and convenient responsiveness,^{19a} since the pioneering work of Stoddart et al..^{19b} Usually, the assembled host-guest architectures were connected by such noncovalent interactions as hydrogen bonding, $\pi\cdots\pi$ stacking, charge transfer, and hydrophobic interactions, which leads not only to good binding affinity, but also to the formation of complexes with a fixed host-guest geometry and directionality.²⁰⁻²² Especially, hydrogen bonding and $\pi\cdots\pi$ stacking often acting as adhesive and cohesive forces in designing solid-state assembly of anion-templated molecular architectures.^{20b, 21b, 22b}

For the crown ethers-ammonium salts ($R-NH_3^+$) systems, the utilization of the R group as a molecular rotor or pendulum unit to create host-guest supramolecule with desirable properties such as phase change materials or ferroelectric molecular materials have been well developed in the literature.²³ In our previously work,^{24, 25} we have investigated the influence of R group containing carboxyl group (4-methylamino benzoic acid and m-amino benzoic acid) on the supramolecular assembly behaviour of host-guest geometry and directionality of crown ethers (18-C-6, and 15-C-5), and influences of different inorganic anions on the supramolecular structures of crown ether- ammonium cation (2-hydroxypropane-1, 3-diamino, 4-methylaniline and 4-iodoaniline)-inorganic anion ($HClO_4$, and HBF_4) system (Scheme 1). As

part of our systematic studies on crown ethers-ammonium salts systems, in this work, we introduced six different ammonium salts (Scheme 1) into 18-crown-6 and 15-crown-5, and we obtained six host-guest supramolecules (Scheme 2): Pyridine-4-ammonium-18-crown-6-perchlorate ($[(C_5H_7N_2)_2 \cdot (18-C-6)]^{2+} \cdot 2(ClO_4)^-$, **1**), 2-Chloride-pyridine-3-ammonium-18-crown-6-perchlorate ($[(C_5H_6N_2Cl) \cdot (18-C-6)]^+ \cdot (ClO_4)^-$, **2**), Isoniazide-ammonium-18-crown-6-tetrafluoroborate ($[(C_6H_9N_3O)_2 \cdot (18-C-6)_3]^{4+} \cdot 4(BF_4)^- \cdot 4(H_2O)$, **3**), Naphthylammonium-18-crown-6-tetrafluoroborate ($[(C_{10}H_{10}N) \cdot (18-C-6)]^+ \cdot (BF_4)^-$, **4**), Benzidine-ammonium-15-crown-5-tetrafluoroborate ($[(C_{12}H_{14}N_2) \cdot (15-C-5)]^{2+} \cdot 2(BF_4)^-$, **5**), Salicylamide-18-crown-6-tetrafluoroborate ($[(C_7H_6NO_2BF_2) \cdot (18-C-6)]$, **6**). For the ammonium salts in complexes **1-6**, the positions of amino groups turned the conformations of crown ethers and the supramolecular structures, we investigated detailed these influences by single-crystal X-ray diffraction, IR and Raman spectra. We further investigated the influences of different ammonium salts on the intermolecular interactions experienced by crown ethers in the supramolecules by using Hirshfeld surfaces analysis, the latter services as powerful tool for elucidating molecular crystal structures and gaining additional insight into polymorph comparison as well as identifying common features and trends in specific classes of compounds.²⁶⁻³⁰ Thus, the results from Hirshfeld surfaces analysis can give additionally insight into the influences of amino group positions on the conformations of crown ethers quantitatively. It is interesting that the HBF_4 in complex **6** reacted with salicylamide through the substitution of two oxygen atoms on salicylamide with two fluorine atoms. To the best of our knowledge, this kind of reaction is unprecedented.

Scheme 1 List of Ammonium Salts Used for Host-Guest Interactions with Crown Ethers (18-C-6 and 15-C-5) Reported in Present Study (**1-6**) and Our Previously Works (**7-11**)

Scheme 2 Components and Molecular Structures of complexes **1-6**

■ RESULTS AND DISCUSSION

Crystal structures of complexes 1-6.

The RT X-ray single-crystal structure determination reveals that complex **1** ($[(C_5H_7N_2)_2 \cdot (18-C-6)]^{2+} \cdot 2(ClO_4^-)$) crystallizes in the triclinic crystal system with $P-1$ space group while complexes **2-6** are all crystallize in the monoclinic crystal system with $P21/c$ space group. Crystal structures of **1-6** were shown Fig. 1-Fig. 5 and hydrogen bonding interactions were tabulated in Table 1. The asymmetric unit of **1** contains one-half of the 18-crown-6 molecule, one pyridine-4-ammonium cation and one perchlorate ion. The basic unit of **1** was composed of an 18-crown-6 molecule, two pyridine-4-ammonium cations and two perchlorate ions. In its structure, the 18-crown-6 molecule lies on the symmetric plane and acting as a molecular stator, while the pyridine-4-ammonium cation and perchlorate ion located on two sides of it can be treated as the molecular rotor (Fig. 1 a). The molecular rotors connect to molecular stators through N-H \cdots O hydrogen bonding interactions (N \cdots O distance 3.038 (12)), and the perchlorate ions look like a pendulum to swing around the axis of the pyridine-4-ammonium cation through N-H \cdots O hydrogen bonding interactions (average N \cdots O distance 3.032 (12)). It is proposed that the pendulum-like molecular motion of **1** is similar with the reported complex potassium hydrogen bis(dichloroacetate)-18-crown-6.²³

Fig. 1 a: The connecting motif of the basic unit for complex **1**; b: The 1D chain packing motif of the basic units along a axis, and the adjacent stacked by $\pi\cdots\pi$ interactions; c: Trochal motif of 1D chain for complex **1** along b axis; d: The cross-linking motif of different 1D chains along b axis into 2D structure.

The pendulum-like units in **1** first packed parallel into 1D linear chain along a axis (Fig. 1 b), and 1D linear chain displays trochal-like motif when viewed from b axis. Then the different 1D chains are stacked interlaced by slight $\pi\cdots\pi$ interactions between pyridine-4-ammonium cations in different chains with centroid-centroid distances of 5.655 Å (Fig. 1 b, d). The symmetry of the 18-crown-6 in **1** was encountered nearly ideal crown "round" " D_{3d} like" conformation, where oxygen atoms (O5, O6, O8, O5A, O6A, O8A) of

the 18-crown-6 in the structure are co-plane with $rms = 0.0000$. The N2 atom on pyridine-4-ammonium cation is lying $0.2514 (15) \text{ \AA}$ higher from the best plane of the oxygen atoms of the crown ring.

Shown in Fig. 2 were the crystal structures of complex **2** ($[(C_5H_6N_2Cl) \cdot (18-C-6)]^+ \cdot (ClO_4)^-$), the asymmetric unit of **2** contains one 18-crown-6 molecule, one 2-chloride-pyridine-3-ammonium cation and one perchlorate ion. For the 2-chloride-pyridine-3-ammonium cation, the amino group is located in *m*-position of the nitrogen atoms on pyridine ring and leads to the protonation of amino group, which is different from complex **1**. The basic unit of **2** is composed of a umbrella-like 2-chloride-pyridine-3-ammonium-18-crown-6 complex cation and a perchlorate ion, the complex cation is connected by six different N-H...O hydrogen bonding interactions and the perchlorate ion is located on the opposite position of the chloride atom on the pyridine ring (Fig. 2 a). The different basic units first packed into 1D linear chain in "A(-A)A(-A)" fashion along *c* axis (Fig. 2 a), and it looks like a "Chinese knot" when viewed from *b* axis (Fig. 2 b). The different "Chinese knots" further stacked paralleled into 3D motif. The conformation of the 18-crown-6 in **2** is a distorted "boat-like" rather than " D_{3d} like" conformation, which is significantly different from **1**. For the distorted "boat-like" conformation, the both ends of the "boat" are occupied by O5 and O10 atoms, which deviate $0.546 (20)$ and $0.6541 (19) \text{ \AA}$ above the mean O-atom plane (rms deviation = 0.4910) of 18-crown-6, respectively. Atoms O6, O7, O8 and O9 are located on the bottom of "boat" and deviate $0.5562 (19)$, $0.0352 (22)$, $0.0401 (18)$ and $0.639 (21) \text{ \AA}$ below the mean O-atom plane, respectively. The N2 atom of the 2-chloride-pyridine-3-ammonium cation is lying $1.0604 (25) \text{ \AA}$ from the best plane of the oxygen atoms of the crown ring.

Fig. 2 a: The 1D packing motif of complex **2** with the crown-ammonium salt unit in "A(-A) A(-A)" packing fashion along *c* axis; **b:** The 3D stacking motif of different 1D chains for complex **2** along *b* axis.

Complex **3** ($[(C_6H_9N_3O)_2 \cdot (18-C-6)_3]^{4+} \cdot 4(BF_4)^- \cdot 4(H_2O)$) is significant different from **1** and **2** due to the

longer distances between nitrogen atoms on pyridine ring and amino group than in the latter two, Fig. 3 shown the crystal structures of it. The asymmetric unit of **3** contains one and one-half of the 18-crown-6 molecules, one isoniazide-ammonium cation, two tetrafluoroborate ions and two solvent water molecules. The basic unit of **3** is composed of three 18-crown-6 molecules, two isoniazide-ammonium cation, four tetrafluoroborate ions and four solvent water molecules (Fig. 3 a). In its structure, both the nitrogen atoms (N3) on pyridine ring and amino group (N1) are protonated, and both are connected to 18-crown-6 molecule through two and six different N-H...O hydrogen bonding interactions, respectively, with every amino group (N1) binds to one 18-crown-6 molecule and two nitrogen atoms (N3) on pyridine ring bind to one 18-crown-6 molecule symmetrically. The 18-crown-6 molecule that binds to N3 atom displays a distorted "chair-like" conformation, with the "foot" (O13, O14) and "head" (O13A, O14A) of the "chair-like" conformation connect to N3 atom with deviation of 0.0003 (1) Å below and above the mean O-atom plane (*rms* deviation = 0.0004), O12 atom deviate 0.0006(1) Å below the mean O-atom plane. While the 18-crown-6 molecule which connected to N1 atom displays an ideal "round" " D_{3d} like" conformation, with the oxygen atoms of 18-crown-6 molecule displaced alternately above and below the media plane of the ring, forming two approximately parallel and nearly equilateral triangles. Where, O7, O9 and O11 atoms located 0.2962 (34), 0.2142 (34) and 0.0829 (31) Å above the mean O-atom plane (*rms* deviation = 0.2164), respectively, and O6, O8 and O10 atoms located 0.1769 (29), 0.3139 (35) and 0.1026 (32) Å below the mean O-atom plane, respectively. The N1 and N3 atoms of the isoniazide-ammonium cation are lying 0.8493 (39) and 2.3828 (98) Å from the best plane of the oxygen atoms of the crown ring, respectively. The solvent water molecules, which bind to N2 atom on the isoniazide-ammonium cation through O-H...N hydrogen bonding interactions, can be treated as molecular rotor with all the 18-crown-6 molecules act as molecular stator. To the best of our knowledge, this kind of pendulum-like motif with three stators and two rotors is unprecedented. The basic unit of **3**, which stacked into infinite 3D structures, adopts two orientations (A and B) in the crystal (Fig. 3 b).

Fig. 3 a: The connecting motif of the three crown ethers components unit for complex **3**; b: The stacking motif of different three crown ethers units in **3** with two different orientations (A and B).

Shown in Fig. 4 were the crystal structures of complex **4** ($[(C_{10}H_{10}N) \cdot (18-C-6)]^+ \cdot (BF_4)^-$), which is similar with **2**. The asymmetric unit of **4** contains one 18-crown-6 molecule, one naphthylammonium cation and one tetrafluoroborate ion. The umbrella-like complex cation is connected by six different N-H \cdots O hydrogen bonding interactions (Fig. 4 a), and the conformation of 18-crown-6 molecules in **4** is a distorted “boat-like” conformation that similar with **2**. The both ends of the “boat” are occupied by O3 and O6 atoms, which deviate 0.6397 (18) and 0.5959 (21) Å above the mean O-atom plane (*rms* deviation = 0.4658) of 18-crown-6, respectively. Atoms O1, O2, O4 and O5 are located on the bottom of “boat” and deviate 0.0868 (20), 0.5203 (19), 0.1391 (18) and 0.4895 (21) Å below the mean O-atom plane, respectively. The N1 atom of the naphthylammonium cation is lying 1.0903 (26) Å from the best plane of the oxygen atoms of the crown ring.

The asymmetric unit of **4** forms a reversely symmetry double units (Fig. 4 a), with centroid-centroid distances between naphthalene ring is 8.025 Å. In the crystal, the countless reversely symmetry double units stacked into 3D motif with two different orientations (Fig. 4b).

Fig. 4 a: The reversely symmetry assembly unit of complex **4**; b: The stacking motif of different reversely symmetry assembly units in **4** with two different orientations (A and B), the BF_4^- ions were omitted for clarity.

Shown in Fig. 5a and 5b were the crystal structures of complex **5** ($[(C_{12}H_{14}N_2) \cdot (15-C-5)]^{2+} \cdot 2(BF_4)^-$), the 15-crown-5 was used. The asymmetric unit of **5** contains one molecule of 15-crown-5, one-half of a benzidine-ammonium cation and one tetrafluoroborate ion. The basic unit can be treated as two reversely symmetry asymmetric “dumbbell-like” units, with two 15-crown-5 molecules hang on the two ends of

benzidine-ammonium salt through four N-H...O hydrogen bonding interactions. The 15-crown-5 molecule in complex **5** encountered nearly “chair like” conformation with O1, O3, O4, and O5 form a mean O-atom plane (O1 and O4 atoms are located above the mean O-atom plane (*rms* deviation = 0.1474) with distances 0.1054 (15) and 0.1807 (25) Å, O3 and O5 atoms are below the plane with distances 0.1096 (16) and 0.1765 (25) Å, respectively), and O2 atom was located 0.9614 (62) Å lower from the plane. The N1 atom of the benzidine-ammonium cation is in the perching position, lying 1.5686 (43) Å higher from the best plane of the oxygen atoms of the crown ring, rather than in the nesting position. The basic unit of **5** paralleled into 1D unit with plane separation of 5.912 Å, the 1D units further stacked paralleled into 3D motif with tetrafluoroborate ion fill in the void between 1D units (Fig. 5 a).

Fig. 5 a:: The 3D stacking motif of different 1D chains for complex **5**; **b**: The 2D stacking motif of complex **6** with 1D structures stacked in “A(-A)A (-A)” fashion along *c* axis.

The crystal structure of complex **6** ($[(C_7H_6NO_2BF_2) \cdot (18-C-6)]$) was shown in Fig. 5b, it is interesting because the tetrafluoroboric acid reacted with salicylamide and give birth to a novel complex (Scheme 3). This novel complex connected to 18-crown-6 molecule through N-H...O hydrogen bonding interactions to form the basic unit of **6**, this basic unit paralleled along *c* axis into 1D chain structure, and the different 1D chains stacked in “A(-A)A(-A)” fashion (Fig. 5b). The 18-crown-6 molecule in complex **6** displays an ideal “round” “ D_{3d} like” conformation, with O2, O4, and O6 atoms located 0.1833 (13), 0.2640 (15) and 0.2438 (15) Å above the mean O-atom plane (*rms* deviation = 0.2328), respectively, and O1, O3, and O5 atoms located 0.1912 (14), 0.2283 (15) and 0.2717 (14) Å below the mean O-atom plane, respectively. The N1 atom of the salicylamide molecule are lying 1.4314 (25) Å from the best plane of the oxygen atoms of the crown ring.

Scheme 3 The synthetic route for complex **6**.

Table 1 Geometrical parameters for hydrogen bonds in complexes **1-6**

Compound d	D–H…A	D–H (Å)	H…A (Å)	D…A (Å)	∠D–H…A(deg)	symmetry operation
1	N1–H1A…O2	0.86	2.08	2.880(15)	154	x, 1+y, -1+z
	N1–H1A…O2'	0.86	2.18	3.038(12)	172	x, 1+y, -1+z
	N1–H1B…O1	0.86	2.38	3.179(8)	154	1-x, 1-y, 1-z
	N2–H2…O5	0.92	1.93	2.808(6)	159	x-1,y,z
2	N2–H2A…O5	0.89	2.57	2.868(4)	101	
	N2–H2A…O6	0.89	2.04	2.921(4)	174	
	N2–H2A…O8	0.89	2.54	2.985(4)	112	
	N2–H2B…O10	0.89	1.94	2.825(4)	178	
	N2–H2C…O7	0.89	1.94	2.823(4)	171	
3	N1–H1A…O8	0.89	2.09	2.827(7)	140	1-x, -1/2-y, 1/2-z
	N1–H1A…O9	0.89	2.19	2.897(7)	136	1-x, -1/2-y, 1/2-z
	N1–H1B…O10	0.89	2.13	2.801(7)	132	1-x, -1/2-y, 1/2-z
	N1–H1B…O11	0.89	2.12	2.888(5)	144	1-x, -1/2-y, 1/2-z
	N1–H1C…O6	0.89	2.2	2.934(6)	139	1-x, -1/2-y, 1/2-z
	N1–H1C…O7	0.89	2.33	3.006(6)	133	1-x, -1/2-y, 1/2-z
	N3–H3A…O14	0.99	1.89	2.774(7)	147	x,-1/2+y, 3/2-z
	N3–H3A…O13	0.99	2.36	3.061(7)	127	x, 3/2-y, -1/2+z
	O15–H15C…N2	0.82	1.94	2.737(6)	164	
	O15–H15D…F7	0.82	2.4	3.081(8)	142	x, 1+y, z
O16–H16C…O15	0.82	2.39	2.792(10)	111		
4	N1–H1A…O1	0.89	2.07	2.939(3)	165	
	N1–H1A…O2	0.89	2.45	2.989(3)	119	
	N1–H1B…O5	0.89	2.12	2.975(3)	162	
	N1–H1B…O6	0.89	2.5	2.900(4)	108	
	N1–H1C…O3	0.89	2.05	2.930(3)	171	
	N1–H1C…O4	0.89	2.57	3.034(3)	113	
5	N1–H1C…F1	0.89	1.91	2.747(8)	156	x-1,y,z
	N1–H1D…O1	0.89	2.07	2.941(6)	168	x-1,y,z
	N1–H1D…O5	0.89	2.47	2.950(6)	114	x-1,y,z
	N1–H1E…O3	0.89	2.02	2.909(7)	172	x-1,y,z
	N1–H1E…O4	0.89	2.55	2.955(6)	108	x-1,y,z
6	N1–H1A…O3	0.86	2.09	2.931(3)	166	1-x,-1/2+y,1-z
	N1–H1B…O1	0.86	2.21	3.056(3)	169	1-x,-1/2+y,1-z

Hirshfeld Surfaces Analysis

The 3D Hirshfeld surfaces and 2D fingerprint plots are unique for any crystal structures, they serve as powerful tools for gaining additional insight into crystal structure comparison by color-coding short or long contacts. The 2D fingerprint plots, which derive from 3D Hirshfeld surfaces, can give a quantitative summarization of the nature and type of intermolecular contacts experienced by the molecules in the

crystal at the same time, it can further be broken down to give the relative contribution to the Hirshfeld surface area from each type of interactions presented, quoted as the “contact contribution”. In this work, we performed Hirshfeld surfaces on crown ethers in complexes **1-6** to investigate quantitatively the influences of different ammonium salts on the intermolecular interactions.

The 3D Hirshfeld surfaces and 2D fingerprint plots of 18-crown-6 and 15-crown-5 in complexes **1-6** were shown in the Fig. 6, there are two different kinds of 18-crown-6 molecules in complex **3** were distinguished as 3 (“ D_{3d} like” conformation) and 3’ (“chair like” conformation). Clearly shown in Fig. 6 were the similarities and differences of the influences of different ammonium salts on the intermolecular interactions of the crown ether molecules. The red dots on the Hirshfeld surfaces are corresponding to the N-H...O hydrogen bonding interactions, the blue area are refer to the C-H contacts and green area are corresponding to H-H contacts. From Fig. 6, the intermolecular interactions experienced by crown ethers in complexes **1-6** are dominated by H-H, O-H, and C-H contacts. The H-H contacts, which are reflected in the middle of scattered points in the 2D fingerprint plot, have the most significant contribution to the total Hirshfeld surfaces of crown ethers in complexes **1-6**, with contributions comprise 51.3, 52.1, 55.9, 51.6, 54.8, 58.6, and 61.6 % to the total Hirshfeld surfaces of complexes **1-6**, respectively (Summarized in Fig. 7). The N-H...O hydrogen bonding interactions, which appear as sharp spikes in the bottom right of the 2D fingerprint plots, represent the closest contacts and comprise 41.7, 35.7, 24.5, 19.9, 18.3, 17.2, and 20.2 % to the total Hirshfeld surfaces. The C-H... π interactions, which are indicated by the “wings” in the upper left and lower right of the 2D fingerprint plot, comprise 4.9, 4.3, 2, 11.1, 5.3, and 5.9 % to the total Hirshfeld surfaces. Apart from these above, the presence of N-H contacts in complexes **1-3**, **5**, and **6**; C-N contacts in complexes **1** and **2**; and O-C contacts in complexes **1-4**, and **6** are observed and all been summarized in Fig. 7.

Fig. 6 3D d_{norm} surfaces and 2D fingerprint plots of crown ethers in complexes **1-6**.

Fig. 7 Relative contributions of various intermolecular contacts to the Hirshfeld surface area in **1-6**.

The different ammonium salts have slight influences on the H-H contacts experienced by crown ethers in complexes **1-6**, but have significant influences on the O-H and N-H contacts. For complex **3**, the H-H and O-H contacts for “ D_{3d} like” conformation are larger than for “chair like” conformation, while C-H... π contacts are identical for them. The O-H contacts are decreased successively for complexes **1-6** due to the increasing of steric hindrance around amino groups in ammonium salts. For complex **4**, the superior conjugation property of naphthylammonium cation leads to the highest contribution of C-H... π contacts. Additionally, for the crown ethers with “chair-like” conformation (**3'** and **5**), there are no voids within the 3D Hirshfeld surfaces and have the closest H-H contacts with $d_e + d_i = 2.2$ on the 2D fingerprint plots.

Raman spectra of complexes **1-6**

Shown in the Fig. 8 were the Raman spectra of 18-crown-6, 15-crown-5 and complexes **1-6** in the region of 400-3500 cm^{-1} . The characteristic peaks for 18-crown-6 are located in the regions between 2800 and 3100 cm^{-1} , and between 1500 and 400 cm^{-1} . Complex formation of 18-crown-6 with ammonium salts caused significant influences on the characteristic peaks of 18-crown-6, the influences on the region between 2800 and 3100 cm^{-1} were highlighted in Fig. 8 upside, and the influences on the region between 1500 and 400 cm^{-1} were highlighted in Fig. 8 bottom. For the region between 2800 and 3100 cm^{-1} , pyridine-4-ammonium salt (**1**) almost leads to the vanish of 18-crown-6 characteristic peaks between 2800 and 3100 cm^{-1} ; 2-chloride- pyridine-3-ammonium salt (**2**) causes the blue shift of these characteristic peaks to 2500-3000 cm^{-1} ; the isoniazide-ammonium salt (**3**) and naphthylammonium salt (**4**) are all lead to the vanish of 18-crown-6 characteristic peaks between 2928 and 2800 cm^{-1} while maintain the characteristic peak at 2950 cm^{-1} ; the novel complex in **6** caused opposite results when compared with isoniazide- ammonium salt and naphthylammonium salt, it leads to the vanish of 18-crown-6 characteristic peak at 2950 cm^{-1} but maintains the peaks between 2928 and 2800 cm^{-1} . While for 15-crown-5, there are only three

characteristic peaks at around 558, 1097 and 2389 cm^{-1} , and they are almost vanished when complexation with benzidine-ammonium salt.

For the region between 1500 and 400 cm^{-1} , we were highlighted the influences of different ammonium salts on the characteristic peaks of 18-crown-6 at six different wavenumbers. The peak at 418 cm^{-1} and the three peaks between 900 and 800 cm^{-1} may belong to characteristic peaks for 18-crown-6 with “round” “ D_{3d} like” conformation. For complexes **1** and **6**, these two characteristic peaks are maintained due to the presences of “ D_{3d} like” conformation, while for complexes **2** (“boat form” conformation), **3** (“chair-like” conformation) and **4** (“boat form” conformation), the peak at 418 cm^{-1} was vanished and the three peaks between 900 and 800 cm^{-1} were reduced to two (**2** and **3**) and one (**4**), respectively. Additionally, the characteristic peak at 583 cm^{-1} for 18-crown-6 was vanished in the presence ammonium salts, the three peaks within 1410- 1500 cm^{-1} were reduced to one for complexes **1** and **6**, and two for complexes **2-4**, the two peaks at 1136 and 1160 cm^{-1} were vanished for complexes **1** and **6**, and reduced to one for complexes **2-4**. From these results above, the ammonium salts lead to different changes on Raman spectra for 18-crown-6 with different conformations.

Fig. 8 Raman spectra of complexes **1-6**, the influences of different ammonium salts on crown ethers were highlighted

IR spectra of complexes 1-6

Shown in Fig. 9 were the IR spectra of 18-crown-6, 15-crown-5 and complexes **1-6** in 4000-500 cm^{-1} region, which have provided similar results as Raman spectra. The characteristic peak of 18-crown-6 at 3455 cm^{-1} were undergo blue shift in the presence of ammonium salts to 3439, 3372, 3397, 3394, and 3417 cm^{-1} for complexes **1-4** and **6**, respectively (Fig. 9 upside), and the degree of blue shift is more slight for “ D_{3d} like” conformation than for other conformations. The characteristic peak of 18-crown-6 at 2895 cm^{-1}

was almost maintained in complexes **1-4** and **6** (Fig. 9 upside).

Highlighted in Fig. 9 bottom were the IR spectra of 18-crown-6, 15-crown-5 and complexes **1-6** in 2200-450 cm^{-1} region. The characteristic peak of 18-crown-6 at 1972 cm^{-1} was vanished for complexes **1** and **6** while shift to 1931, 1969, and 2009 cm^{-1} for complexes **2**, **3**, and **4**, respectively. The characteristic peak of 18-crown-6 at 1476 cm^{-1} was maintained for complexes **1**, **2**, **4** and **6** while vanished in complex **3**. The broad peak of 18-crown-6 within the region 1130-1090 cm^{-1} , which was narrow down to 1120-1090 cm^{-1} and 1117-1081 cm^{-1} for complexes **1** and **6**, respectively, was broaden to 1150-1080 cm^{-1} , 1150-1060 cm^{-1} and 1170-1010 cm^{-1} for complexes **2**, **3** and **4**, respectively. For 15-crown-5, the IR spectra of it was similar with 18-crown-6, and complex formation of it with benzidine-ammonium salt lead to broaden of the broad peak from 1130-1120 cm^{-1} to 1132-1078 cm^{-1} . These results again demonstrated the fact that the ammonium salts lead to different changes on Raman spectra for 18-crown-6 with different conformations.

Fig. 9 IR spectra of complexes **1-6**, the influences of different ammonium salts on crown ethers were highlighted.

Conclusions

In conclusion, complex formation of 18-crown-6 with pyridine-4-ammonium salt (**1**)、2-chloride-pyridine-3-ammonium salt (**2**)、isoniazide-ammonium salt (**3**)、naphthylammonium salt (**4**) and salicylamide-difluoroborate (**6**) as well as 15-crown-5 with benzidine-ammonium salt (**5**) have been investigated detailed in this work by single-crystal X-ray diffraction, Hirshfeld surfaces analysis, Raman and IR spectra. Complexes **1** and **3** formed five- and nine-member pendulum-like structures, respectively, with 18-crown-6 acting as molecular stator and ammonium cation or solvent water molecules acting as the molecular rotor. Complexes **2** and **4** formed umbrella-like structures with 18-crown-6 acting as the cover

and ammonium salt act as hand shank of the umbrella. Complex **5** formed “dumbbell-like” structure with 15-crown-5. Complex **6** was interesting because salicylamide formed a novel complex with tetrafluoroboric acid. The conformations of 18-crown-6 in complexes **1** and **6** were “round” “ D_{3d} like” while display “boat-form” in complexes **2** and **4**. There are two different conformations of 18-crown-6 in complexes **3** with “round” “ D_{3d} like” and “chair-like” conformations in stoichiometric of 2:1. The conformations of crown ethers lead to different intermolecular interactions and spectroscopic properties, for example: the “ D_{3d} like” conformation is more apt to H-H and O-H contacts than for “chair like” conformation, and the latter is apt to C-H... π contacts; the characteristic Raman peaks at 418 cm^{-1} and between 900 and 800 cm^{-1} are maintained for “ D_{3d} like” conformation while vanished for “boat-like” and “chair-like” conformation; the characteristic IR peak within the region $1130\text{-}1090\text{ cm}^{-1}$ was narrowed down for “ D_{3d} like” conformation while broadened for other conformations. These results are important not only for the evaluation of the specific case of the 18-crown-6-ammonium system, but also for other host-guest systems where multiple conformations of the host molecule are possible.

EXPERIMENTAL SECTION

Materials and Physical Measurements

18-crown-6, 15-crown-5, pyridine-4-amino 2-chloride- pyridine-3-amino, isoniazide, naphthyl-1-amino, benzidine, salicylamide, HClO_4 and HBF_4 were all commercially available from Sigma Aldrich and used as received without further purification. Methanol was commercially available from Sinopharm Chemical Reagent Co., Ltd and used as received without further purification. Elemental analyses were performed by a Vario-EL III elemental analyzer for carbon, hydrogen, and nitrogen of the complexes **1-6**. Infrared spectra were recorded on a SHIMADZU IR prestige-21 FTIR-8400S spectrometer in the spectral range $4000\text{-}500\text{ cm}^{-1}$, with the samples in the form of potassium bromide pellets. Raman spectra were recorded using a Raman microscope (Kaiser Optical Systems, Inc., Ann Arbor, MI, USA) with 785 nm laser excitation. The spectra were obtained for one 2 min exposure of the CCD detector in the wavenumber range $50\text{-}3500\text{ cm}^{-1}$.

Preparations of the Complexes

The preparations of complexes **1-6** were performed by slow evaporation technique, 35 mL methanol/water (2:1 v/v) system were used. They all obtained from methanol/water solvent system by a 1:1:1 (0.4 mmol) stoichiometric mixtures of 18-crown-6 (15-crown-5), organic amines (pyridine-4-amino 2-chloride-pyridine-3-amino, isoniazide, naphthyl-1-amino, benzidine and salicylamide) and Inorganic acids (HClO₄ and HBF₄). Single crystals of complexes **1-6** suitable for X-ray diffraction were obtained within four weeks. Complex **1**, elemental analysis Anal. Calcd. (%): C, 40.43; N, 8.59; H, 5.86. Found: C, 40.30; N, 8.48; H, 5.41. IR (KBr, cm⁻¹): 3439, 3349, 3244, 3112, 2888, 2674, 1628, 1591, 1527, 1469, 1351, 1191, 1110, 960, 838, 624, 502. Complex **2**, elemental analysis anal. Calcd. (%): C, 41.47; N, 5.69; H, 5.93. Found: C, 41.68; N, 5.31; H, 5.76. IR (KBr, cm⁻¹): 3372, 3176, 3244, 2950, 2622, 1931, 1629, 1556, 1469, 1242, 1120, 980, 829, 617. Complex **3**, elemental analysis anal. Calcd. (%): C, 38.73; N, 5.64; H, 6.50. Found: C, 38.57; N, 5.45; H, 6.45. IR (KBr, cm⁻¹): 3397, 2052, 1969, 1742, 1697, 1601, 1500, 1468, 1442, 1114, 1031, 1123, 835, 752, 540, 518. Complex **4**, elemental analysis anal. Calcd. (%): C, 53.34; N, 2.82; H, 6.91. Found: C, 53.37; N, 2.85; H, 6.65. IR (KBr, cm⁻¹): 3394, 2891, 2014, 1931, 1629, 1572, 1514, 1476, 1354, 1242, 1120, 963, 842, 810, 774, 524. Complex **5**, elemental analysis anal. Calcd. (%): C, 48.01; N, 3.50; H, 6.80. Found: C, 48.07; N, 3.35; H, 6.65. IR (KBr, cm⁻¹): 3340, 2976, 2670, 2565, 2622, 1947, 1735, 1610, 1473, 1434, 1360, 1284, 1123, 1040, 944, 861, 755, 701, 621, 528. Complex **6**, elemental analysis anal. Calcd. (%): C, 50.79; N, 3.11; H, 6.73. Found: C, 50.67; N, 3.21; H, 6.55. IR (KBr, cm⁻¹): 3417, 3266, 3112, 2914, 1947, 1729, 1613, 1373, 1219, 1117, 992, 854, 531.

X-ray Crystallographic Study

The single-crystal X-ray diffraction data of the complexes **1-6** were collected at 293 K with graphite-monochromated Mo-K α radiation ($\lambda = 0.071073$ nm) equipped with Rigaku SCXmini diffractometer³¹. The lattice parameters were integrated using vector analysis and refined from the diffraction matrix, the absorption correction was carried out by using Bruker SADABS program with

multi-scan method³². The crystallographic data, data collection, and refinement parameters for complexes **1-6** were given in Table S1. The structures were solved by full-matrix least-squares methods on all F^2 data, and used the SHELXS-97 and SHELXL-97 programs³³ for structure solution and refinement respectively. All non-hydrogen atoms were refined anisotropically and hydrogen atoms were geometrically fixed.

ACKNOWLEDGEMENTS

This work has been Supported by the Scientific Research Foundation of Graduate School of Southeast University (YBJJ1340), Fundamental Research Funds for the Central Universities (CXZZ12_0119), Natural Science Foundation of China (21371031; 21241009) and Prospective Joint Research Project of Jiangsu province (BY2012193).

Notes and references

^a School of Chemistry and Chemical Engineering, Southeast University, Nanjing, 210096, P. R. China. Fax: 86-25-52090614; Tel: 86-25-52090614; E-mail: chmsunbw@seu.edu.cn

† Electronic Supplementary Information (ESI) available: [Crystal data and structure refinement parameters for complexes **1-6**,]. See DOI: 10.1039/b000000x/

1. (a) C. J. Pedersen, *J. Am. Chem. Soc.* 1967, **89**, 7017; (b) J. S. Ritch and T. Chivers, *Angew. Chem., Int. Ed.* 2007, **46**, 4610.
2. (a) B. L. Allwood, N. Spencer, H. Shahriari-Zavareh, J. F. Stoddart and D. J. Williams, *J. Chem. Soc., Chem. Commun.*, 1987, 1064; (b) F. M. Raymo, J. F. Stoddart, *Chem. Rev.*, 1999, **99**, 1643.
3. (a) B. Zheng, F. Wang, S. Y. Dong and F. H. Huang, *Chem. Soc. Rev.* 2012, **41**, 1621; (b) X. Z. Yan, F. Wang, B. Zheng and F. H. Huang, *Chem. Soc. Rev.* 2012, **41**, 6042.
4. (a) C. J. Pedersen and H. K. Frensdorff, *Angew. Chem., Int. Ed.* 1972, **84**, 16. (b) I. Goldberg, J. L. Atwood, J. E. D. Davies and D. D. MacNicol, In *Inclusion Compounds* ;Eds.; Academic Press: London, U.K., 1984, 2, 261; (c) Y. H. Luo and B. W. Sun, *Cryst. Growth Des.* 2013, **13**(5), 2098.

5. (a) P. Burkhard, C. H. Tai, J. N. Jansonius and P. F. Cook, *J. Mol. Biol.* 2000, **303**, 279. (b) Y. H. Luo, C. G. Zhang, B. Xu and B. W. Sun, *CrystEngComm*. 2012, **14**(20), 6860; (c) Y. H. Luo, B. Xu and B. W. Sun, *Journal of Crystal Growth*. 2013, **374**, 88. (d) Y. H. Luo, Y. H. Lu and B.W. Sun, *Inorganica Chimica Acta*. 2013, **404**, 188.
6. (a) M. M. Zhang, D. H. Xu, X. Z. Yan, J. Z. Chen, S. Y. Dong, B. Zheng and F. H. Huang, *Angew. Chem. Int. Ed.* 2012, **51**, 7011; (b) B. Zheng, M. M. Zhang, S. Y. Dong, J. Y. Liu and F. H. Huang, *Org. Lett*, 2012, **14**, 306.
7. (a) D. Braga, M. Gandolfi, M. Lusi, D. Paolucci, M. Polito, K. Rubini and F. Grepioni, *Chem. Eur. J.* 2007, **13**, 5250. (b) C. J. Pedersen and H. K. Frensdorff, *Angew. Chem., Int. Ed.* 1972, **11**, 16.
8. (a) J. M. Lehn, *Supramolecular Chemistry: Concepts and Perspectives*; VCH, Weinheim, Germany, 1995; (b) M. Calleja, S. A. Mason, P. D. Prince, J. W. Steed and C. Wilkinson, *New J. Chem.* 2003, **27**, 28. (c) P. C. Junk, B. J. McCool, B. Moubaraki, K. S. Murray, L. Spiccia, J. D. Cashion and J. W. Steed, *Dalton Trans.* 2002, **6**, 1024; (d) J. L. Atwood, K. T. Holman and J. W. Steed, *Chem. Commun.* (Cambridge, U.K.), 1996, 1401.
9. (a) J. M. Harrington, S. B. Jones, P. H. White and R. D. Hancock, *Inorg. Chem.* 2004, **43**, 4456; (b) J. J. Yan, J. Hu and S. Liu, *Macromolecules*, 2009, **42**, 8451; (c) J. W. Steed and J. L. Atwood, *Supramolecular Chemistry: A Concise Introduction*, Wiley, London, 2000; (d) J. W. Steed, *Coord. Chem. Rev.* 2001, **215**, 171.
10. (a) Z. Ge, J. Hu, F. Huang and S. Liu, *Angew. Chem.* 2009, **121**, 1830; (b) J. M. Dou, X. K. Gao, F. Y. Dong, D. C. Li and D. Q. Wang, *Dalton Trans.* 2004, **18**, 2918. (c) J. H. van Esch and B. L. Feringa, *Angew. Chem.* 2009, **121**, 2351; *Angew. Chem. Int. Ed.* 2009, **48**, 2263.
11. (a) L. Brunsveld, B. J. B. Folmer, E. W. Meijer and R. P. Sijbesma, *Chem. Rev.*, 2001, **101**, 4071. (b) X. Yan, D. Xu, X. Chi, J. Chen, S. Dong, X. Ding, Y. Yu and F. Huang, *Adv. Mater.* 2012, **24**, 362.

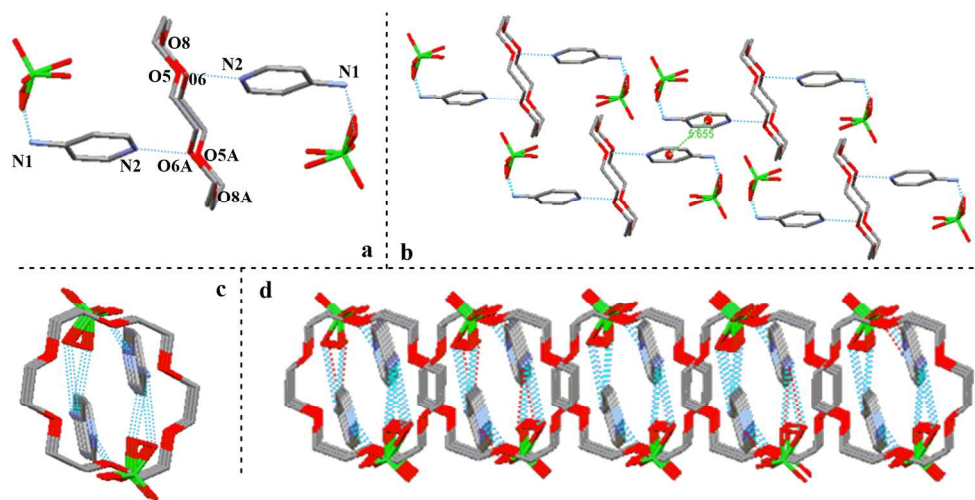
12. (a) T. F. A. De Greef, M. M. J. Smulders, M. A. Wolffs, P. H. J. Schenning, R. P. Sijbesma and E. W. Meijer, *Chem. Rev.*, 2009, **109**, 5687. (b) S. Dong, B. Zheng, D. Xu, X. Yan, M. Zhang and F. Huang, *Adv. Mater.* 2012, **24**, 3191.
13. (a) J. D. Fox and S. J. Rowan, *Macromolecules*, 2009, **42**, 6823. (b) X. Ji, Y. Yao, J. Li, X. Yan and F. Huang, *J. Am. Chem. Soc.* 2013, **135**, 74.
14. S. J. Rowan and J. F. Stoddart, *Polym. Adv. Technol.*, 2002, **13**, 777.
15. R. P. Sijbesma, F. H. Beijer, L. Brunsveld, B. J. B. Folmer, J. H. K. K. Hirschberg, R. F. M. Lange, J. K. L. Lowe and E. W. Meijer, *Science*, 1997, **278**, 1601.
16. W. C. Yount, D. M. Loveless and S. L. Craig, *J. Am. Chem. Soc.* 2005, **127**, 14488.
17. O. Kretschmann, S. W. Choi, M. Miyauchi, I. Tomatsu and A. Harada, H. Ritter, *Angew. Chem.* 2006, **118**, 4468; *Angew. Chem. Int. Ed.* 2006, **45**, 4361.
18. J. H. Lee, H. Lee, S. Seo, J. Jaworski, M. L. Seo, S. Kang, J. Y. Lee and J. H. Jung, *New J. Chem.* 2011, **35**, 1054.
19. (a) F. Wang, C. Han, C. He, Q. Zhou, J. Zhang, C. Wang, N. Li and F. Huang, *J. Am. Chem. Soc.* 2008, **130**, 11254. (b) B. L. Allwood, H. Shahriarizavareh, J. F. Stoddart and D. J. Williams, *J. Chem. Soc., Chem. Commun.*, 1987, 1058.
20. (a) H. Lee, S. H. Jung, W. S. Han, J. H. Moon, S. Kang, J. Y. Lee, J. H. Jung and S. Shinkai, *Chem. Eur. J.* 2011, **17**, 2823. (b) S. K. Seth, P. Manna, N. J. Singh, M. Mitra, A. D. Jana, A. Das, S. R. Choudhury, T. Kar, S. Mukhopadhyay and K. S. Kim, *CrystEngComm*, 2013, **15**, 1285.
21. (a) S. Dong, Y. Luo, X. Yan, B. Zeng, X. Ding, Y. Yu, Z. Ma, Q. Zhao and F. Huang, *Angew. Chem.* 2011, **123**, 1945; *Angew. Chem. Int. Ed.* 2011, **50**, 1905. (b) P. Manna, S. K. Seth, M. Mitra, A. Das, N. J. Singh, S. R. Choudhury, T. Kar and S. Mukhopadhyay, *CrystEngComm*, 2013, **15**, 7879.

22. (a) A. A. Sobczuk, S. -I. Tamaru and S. Shinkai, *Chem. Commun.* 2011, **47**, 3093. (b) A. Das, A. D. Jana, S. K. Seth, B. Dey, S. R. Choudhury, T. Kar, S. Mukhopadhyay, N. J. Singh, I. C. Hwang, K. S. Kim, *J Phys Chem B*, 2010, **114**(12), 4166-70.
23. S. Li, J. Luo, Z. Sun, S. Zhang, L. Li, X. Shi and M. Hong, *Cryst. Growth Des.* 2013, **13**, 2675.
24. (a) Y. H. Luo, W. T. Song, S. W. Ge and B. W. Sun, *Polyhedron*, 2014, **69**, 160. (b) Y.H. Luo, Q.X. Mao and B. W. Sun, *Inorganica Chimica Acta.*, 2014, **412**, 60.
25. (a) Y. H. Luo, S. W. Ge, W. T. Song and B. W. Sun, *New J. Chem.*, 2014, **38**, 723. (b) Y. H. Luo, D. E. Wu, S. W. Ge, Y. Li and B. W. Sun, *RSC Adv.*, 2014, **4**, 11698.
26. (a) S. K. Seth, I. Saha, C. Estarellas, A. Frontera, T. Kar and S. Mukhopadhyay, *Cryst. Growth Des.* 2011, **11**, 3250. (b) S. K. Seth, *CrystEngComm*, 2013, **15**, 1772. (c) S. Adhikari, S. K. Seth and T. Kar, *CrystEngComm*, 2013, **15**, 7372. (d) S. K. Seth, *Journal of Molecular Structure*, 2014, **1064**, 70. (e) S. K. Seth, *Inorganic Chemistry Communications*, 2014, **43**, 60.
27. (a) S. K. Seth, D. Sarkar, A. D. Jana and T. Kar, *Cryst. Growth Des.* 2011, **11**, 4837. (b) S. K. Seth, D. Sarkar and T. Kar, *CrystEngComm*, 2011, **13**, 4528. (c) S. K. Seth, D. Sarkar, A. Roy and T. Kar, *CrystEngComm*, 2011, **13**, 6728.
28. (a) Y. H. Luo, J. Xu and B. W. Sun, *Journal of Chemical Research.* 2012, 36(12), 697; (b) Y.H. Luo, G. G. Wu, S. L. Mao and B. W. Sun, *Inorganica Chimica Acta.* 2013, **397**, 1.
29. (a) Y. H. Luo and B. W. Sun, *CrystEngComm*, 2013, **15**, 7490; (b) Y.-H. Luo, Y. Wang, J. Zhao and Y.-H. Wang, *Spectrochimica Acta Part A: Molecular and Biomolecular Spectroscopy*, 2014, **122**, 246; (c) Y. H. Luo, G. G. Wu and B. W. Sun, *Journal of Chemical Engineering Data.* 2013, **58**, 588; (d) Y. H. Luo, Y. R. Tu, J. L. Ge and B. W. Sun, *Separation Science and Technology.* 2013, **48**, 1881.
30. Y.-H. Luo and B.-W. Sun, *Spectrochimica Acta Part A: Molecular and Biomolecular Spectroscopy*, 2014, **120**, 228; (b) Y. -H. Luo and B. -W. Sun, *Spectrochimica Acta Part A: Molecular and Biomolecular*

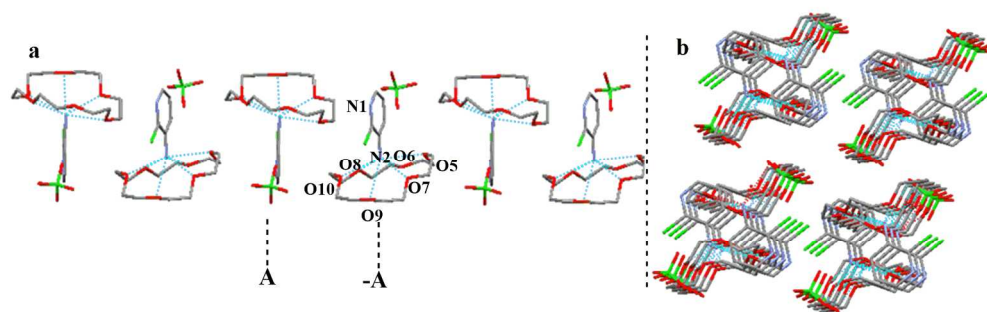
Spectroscopy. 2014, **120**, 381. (c) Y. H. Luo, Q. Zhou and B.W. Sun, *Journal of Chemical Research*.

2012, **36**(9), 506.

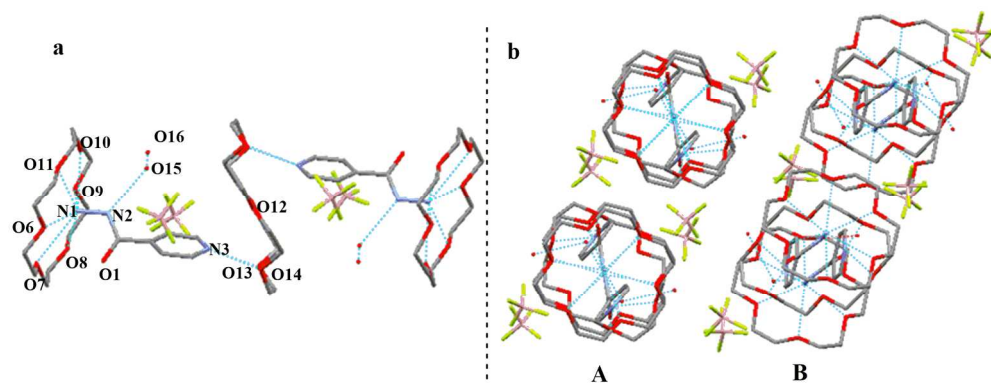
31. Rigaku (2005) CrystalClear, Version 14.0. Rigaku Corporation, Tokyo, Japan.
32. (a) Y. H. Luo and M. L. Pan, *Acta Cryst.* 2012, **E68**, o206. (b) Y. H. Luo, J. Xu, M. L. Pan and J. F. Li, *Acta Cryst.* 2011, **E67**, o2099.
33. G. M. Sheldrick, (1997) SHELXS97: Programs for Crystal Structure Analysis. University of Göttingen, Germany.



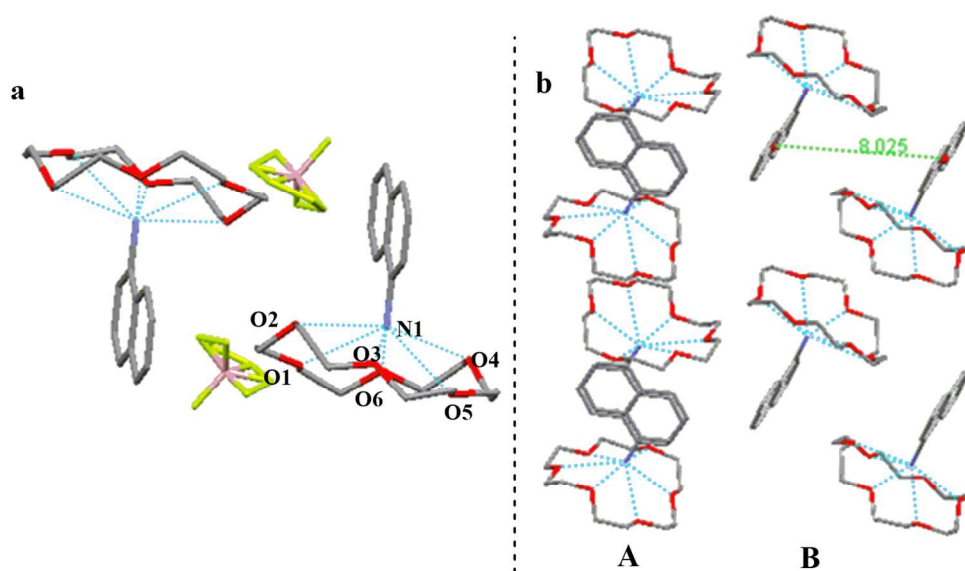
176x90mm (300 x 300 DPI)



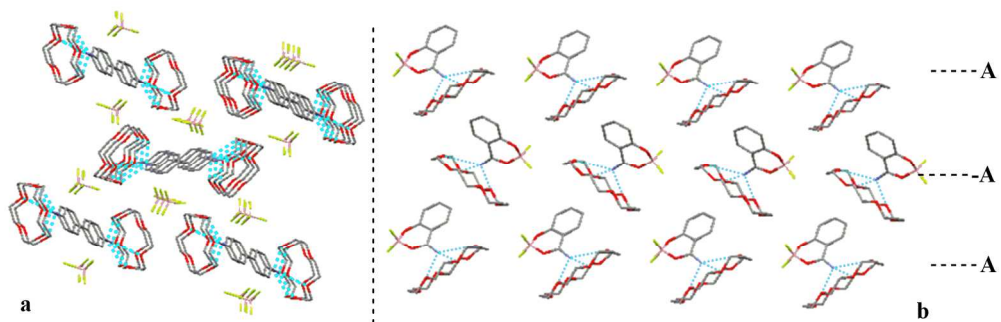
180x58mm (300 x 300 DPI)



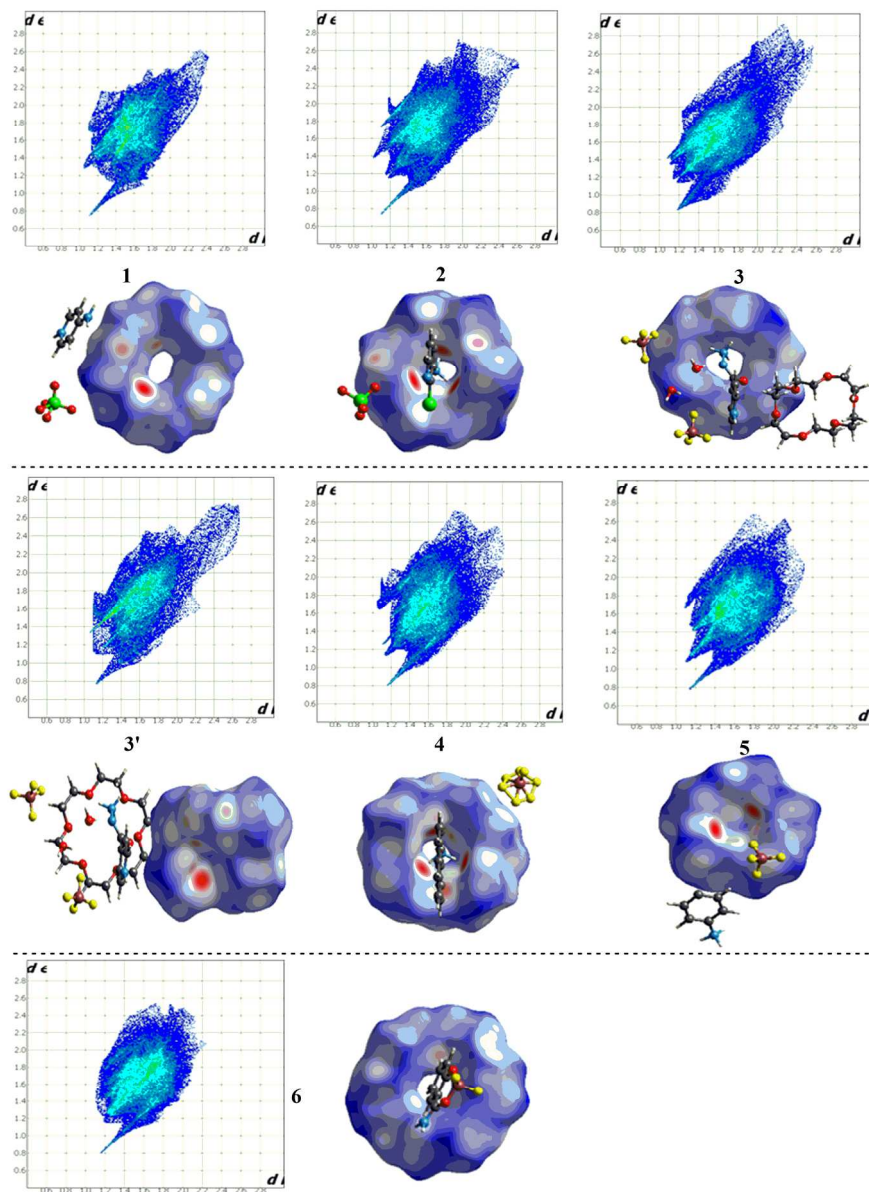
182x71mm (300 x 300 DPI)



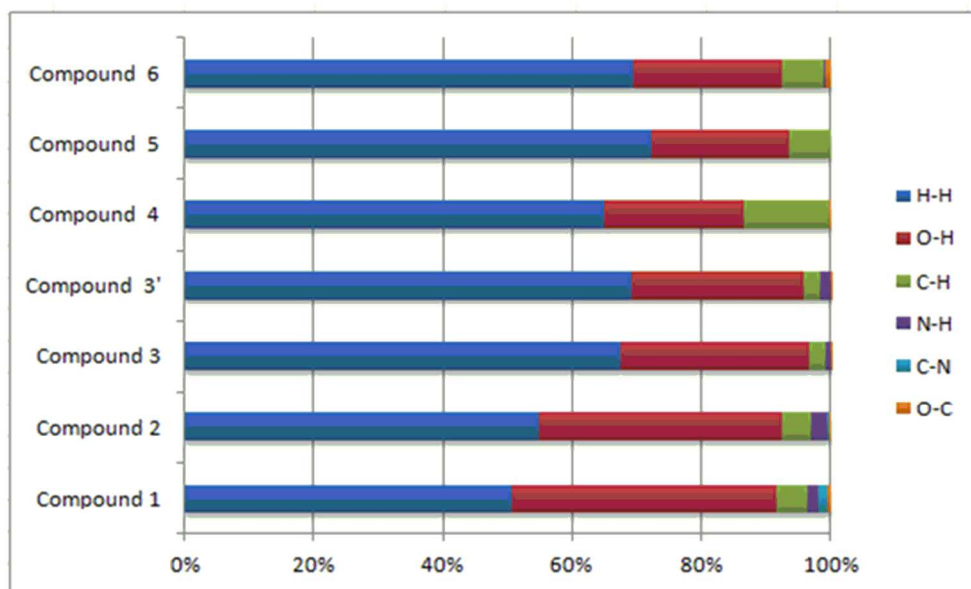
139x81mm (300 x 300 DPI)



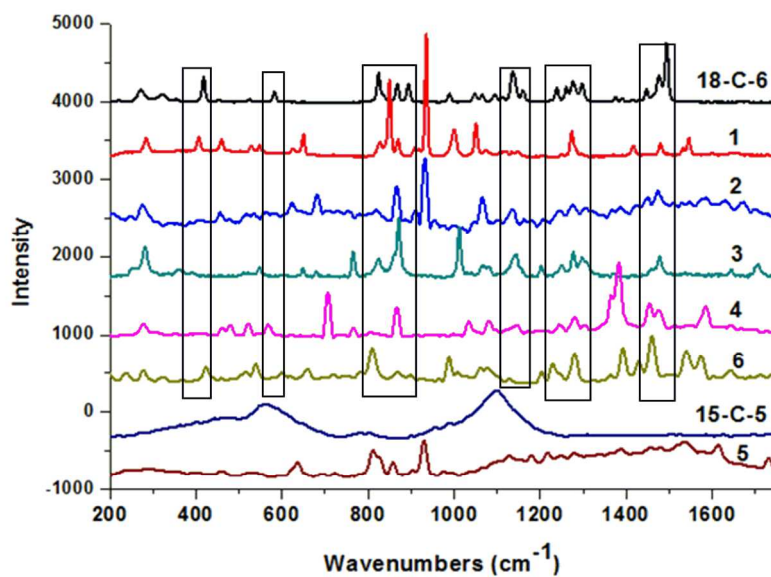
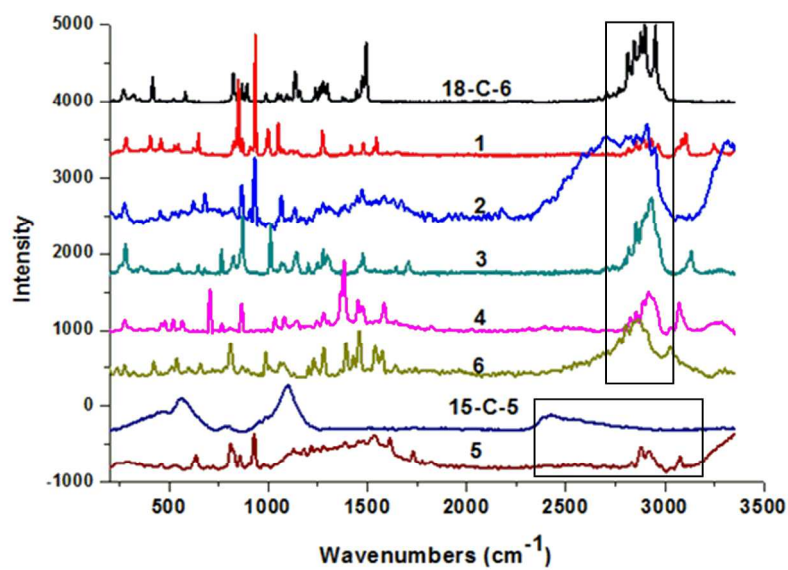
185x60mm (300 x 300 DPI)



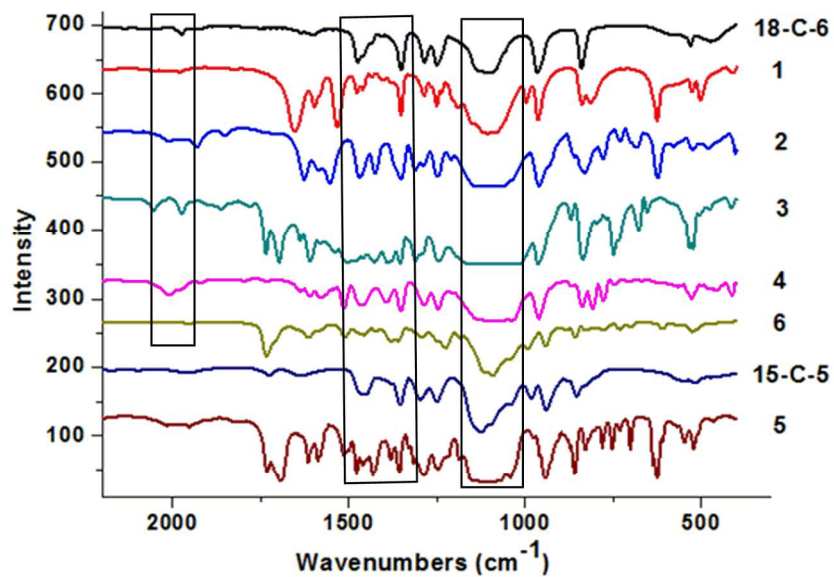
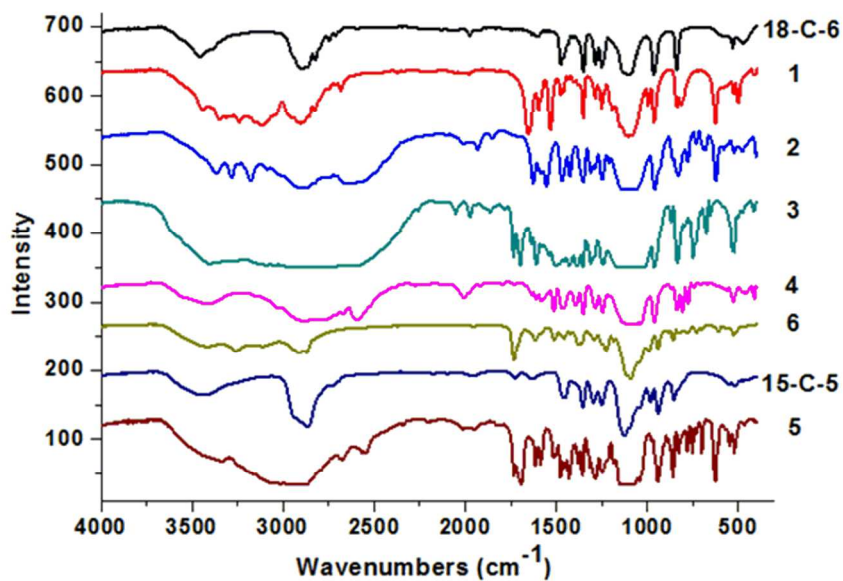
179x241mm (300 x 300 DPI)



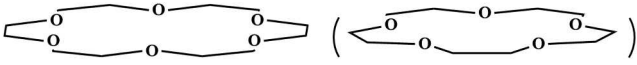
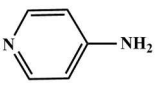
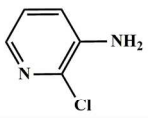
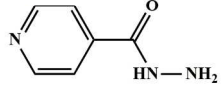
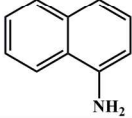
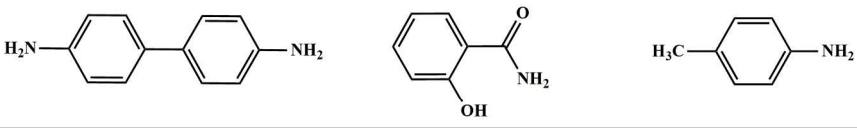
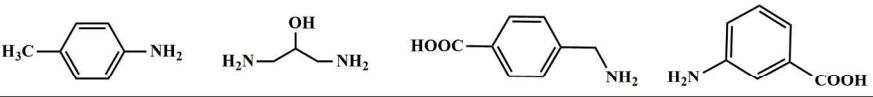
130x80mm (300 x 300 DPI)



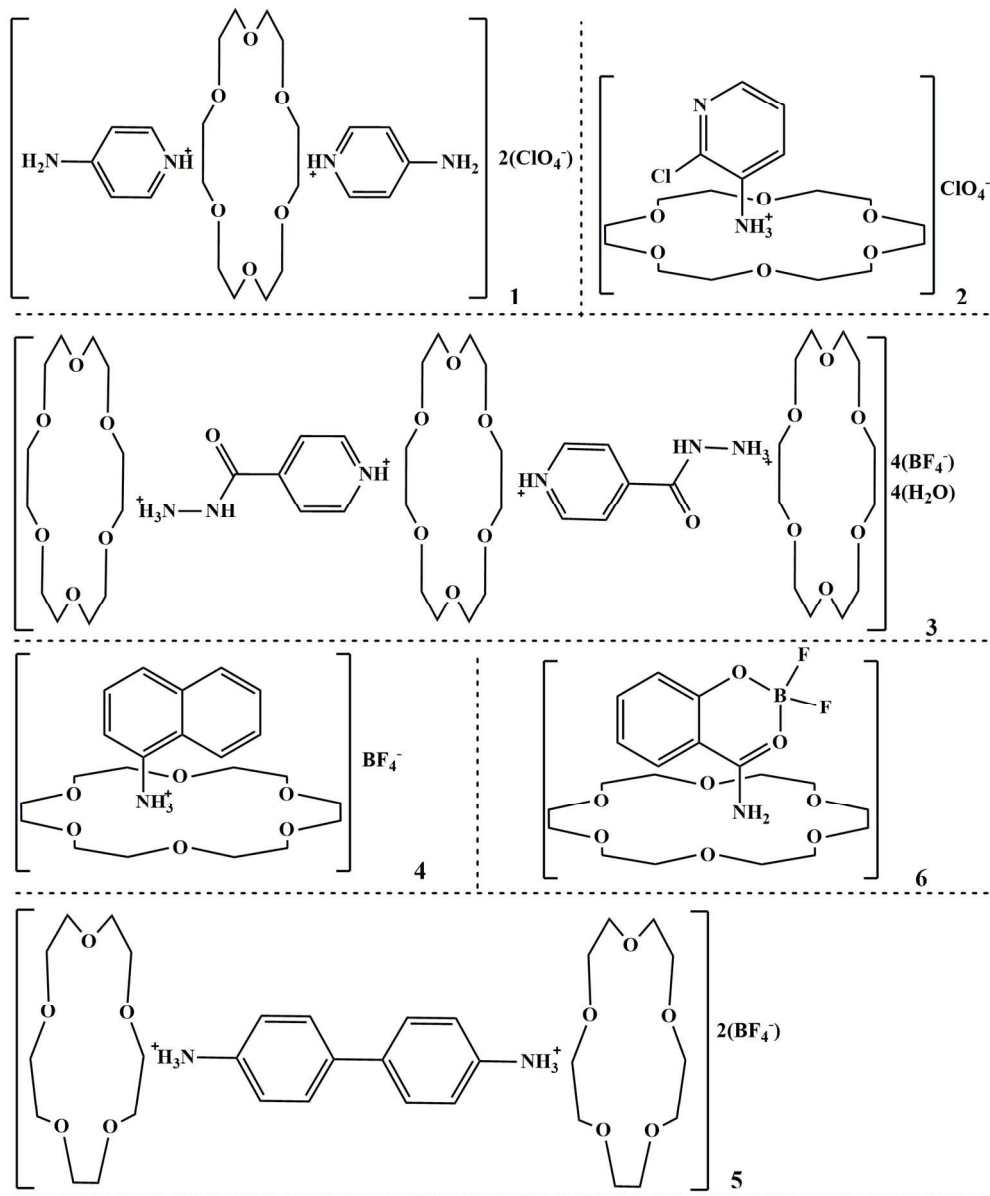
157x229mm (300 x 300 DPI)



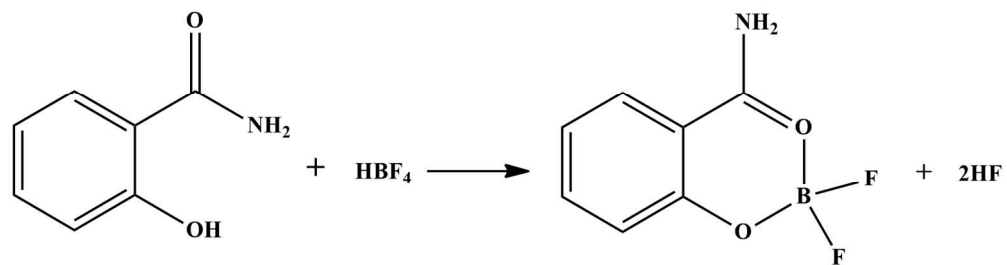
148x207mm (300 x 300 DPI)

			
			
Sl.no	1	2	3
Ref.code	Present study	Present study	Present study
			
Sl.no	5	6	7
Ref.code	Present study	Present study	15
			
Sl.no	8	9	10
Ref.code	15	15	16

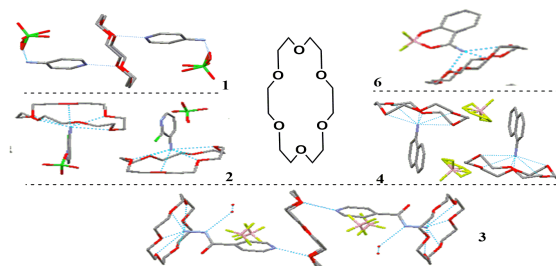
182x119mm (300 x 300 DPI)



149x180mm (300 x 300 DPI)



151x40mm (300 x 300 DPI)



Positions of Amino Groups in Ammonium Salts Turn the Conformations of Crown Ethers